Catalytic Transparency of Hexagonal Boron Nitride on Copper for Chemical Vapor Deposition Growth of Large-Area and High-Quality Graphene

Min Wang,[†,‡] Minwoo Kim,[†,‡] Dorj Odkhuu,[§] Noejung Park,[§] Joohyun Lee,[†,‡] Won-Jun Jang,[∥] Se-Jong Kahng,[∥] Rodney S. Ruoff,[⊥,*] Young Jae Song,[†,‡,#,*] and Sungjoo Lee[†,‡,⊗,*]

[†]SKKU Advanced Institute of Nanotechnology (SAINT), Sungkyunkwan University (SKKU), Suwon 440-746, Korea, [‡]Center for Human Interface Nanotechnology (HINT), Samsung-SKKU Graphene Center, Sungkyunkwan University (SKKU), Suwon 440-746, Korea, [§]Interdisciplinary School of Green Energy and Low Dimensional Carbon Materials Center, Ulsan National Institute of Science and Technology (UNIST), Ulsan 689-798, Korea, [∥]Department of Physics, Korea University, Seoul 136-713, Korea, [⊥]Center for Multidimensional Carbon Materials (CMCM; an Institute for Basic Science (IBS) Center on the UNIST Campus), Department of Chemistry and School of Materials Science, Ulsan National Institute of Science & Technology (UNIST), Ulsan 689-798, Republic of Korea, [#]Department of Physics, Sungkyunkwan University (SKKU), Suwon 440-746, Korea, and [⊗]College of Information and Communication Engineering, Sungkyunkwan University (SKKU), Suwon 440-746, Korea

ABSTRACT Graphene transferred onto h-BN has recently become a focus of research because of its excellent compatibility with large-area device applications. The requirements of scalability and clean fabrication, however, have not yet been satisfactorily addressed. The successful synthesis of graphene/h-BN on a Cu foil and DFT calculations for this system are reported, which demonstrate that a thin h-BN film on Cu foil is an excellent template for the growth of large-area and high-quality graphene. Such material can be grown on thin h-BN films that are less than 3 nm thick, as confirmed by optical microscopy and Raman spectroscopy. We have evaluated the catalytic growth mechanism and the limits on the CVD growth of high-quality and large-area graphene on h-BN film/Cu by performing Kelvin probe force microscopy and DFT calculations for various thicknesses of h-BN.

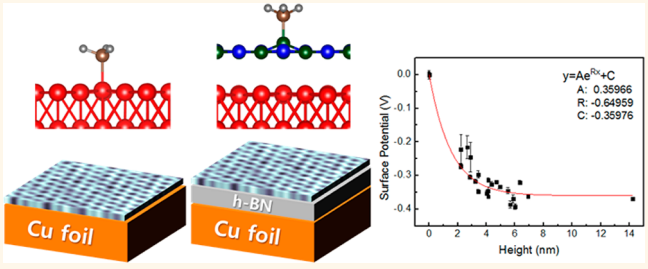

KEYWORDS: graphene · h-BN · direct CVD growth · CVD growth mechanism · catalytic transparency · ideal CVD template

The chemical vapor deposition (CVD) of graphene and hexagonal boron nitride (h-BN) films on transition metal substrates has been shown to yield large-area and high-quality films.[1−8] There has been particular focus on the large-area growth of graphene and h-BN on Cu foil substrates, and a recent study demonstrated the growth of monolayer h-BN on Pt foil.[9] Although the transfer of graphene onto desired substrates such as h-BN can show the quality needed for graphene electronics,[10,11] the process is very tricky and hard to apply for large areas in device applications. The sequential growth of h-BN on a Cu foil followed by graphene is of interest for this reason, and achieving sequential growth (without transfer) would enable the exploration of the possibility of epitaxial growth, which might be beneficial to device performance.[12]

There is also the fascinating possibility that the underlying metal, in this case Cu, could play a role in the catalysis of the formation of a layer of graphene through the thin intermediate h-BN film. Indeed, we show here that when covered with very thin films of h-BN, Cu foil catalyzes the growth of graphene, but that thicker h-BN films impede and essentially prevent the growth of graphene (under the same CVD conditions for graphene growth). The results we present suggest that coating metal catalytic particles (in general, bare metal surfaces, thus protected from oxidation) with ultrathin h-BN films either a monolayer or a few layers thick will open up a new class of catalysts for study and perhaps widespread use for many other reactions.

The growth of graphene has been attempted on various insulators such as

* Address correspondence to yjsong@skku.edu (Y. J. Song), leesj@skku.edu (S. Lee), ruoffrs@gmail.com (R. S. Ruoff).

Received for review September 30, 2013 and accepted May 28, 2014.

Published online May 28, 2014
10.1021/nn501837c

MgO, ZrO_2, SiO_2, and Si_3N_4 but with limited success, yielding nanosized domains with too many defects compared with graphene grown on metal substrates.[13−18] Such direct deposition processes are scientifically intriguing because the graphene CVD growth mechanism is not yet clearly understood. It seems that some dielectrics also provide for the catalytic decomposition of the carbon gas source and for graphene nucleation and growth, although the catalytic effects are weaker than those of their metal counterparts, which means that graphene growth on dielectrics at least to date requires some relatively harsh conditions, such as higher growth temperatures and plasma-enhanced CVD.

A dielectric material of particular interest for graphene applications is h-BN because of its flatness, chemical inertness, low lattice mismatch, and compatibility with graphene. Recently, Liu *et al*. fabricated vertically assembled high-quality graphene/h-BN stacks by carrying out the direct CVD growth of h-BN on graphene by a two-step process.[19] In-plane heterostructures of graphene and h-BN with controlled domain sizes obtained by using lithographic patterning and sequential CVD growth steps have also been reported.[20,21] In a recent study, we found that large-scale monolayer graphene can be directly grown on h-BN/Cu foil by low-pressure CVD and that the direct growth of graphene on h-BN generates a defect-free and clean graphene/h-BN interface, as confirmed with STM/STS, Raman, and electrical carrier transport measurements;[12] however, an explanation of the mechanism of growth of graphene on h-BN/Cu was not presented.

In this study, we address the CVD growth mechanism of large-area and high-quality graphene on h-BN/Cu as an ideal CVD template by measuring the effects of different thicknesses of the h-BN film on graphene growth. As it is difficult to grow CVD graphene on the surfaces of bulk h-BN or thick h-BN films, we studied the dependence of growth on the thickness of the h-BN film for thin films. The presence and quality of the graphene grown on various h-BN/Cu samples were evaluated with Raman spectroscopy. Kelvin probe force microscopy (KPFM) measurements were performed to investigate the electronic influence of h-BN/Cu on graphene growth. Density functional theory (DFT) calculations were made to further understand the CVD growth mechanism of graphene on h-BN/Cu.

RESULTS AND DISCUSSION

The CVD growth of graphene was attempted on h-BN films of different thicknesses on a Cu foil. Figure 1a shows graphene growth on h-BN films of different thicknesses. Thicker h-BN films with consistent quality were prepared by transferring additional h-BN films of the same crystallinity and thickness (Figure 1b). (Note that a film of equal thickness and quality to h-BN for transfer will be designated by "film" and that "atomic layer" indicates a one-atom-thick layer of h-BN in this article.)

In our low-pressure CVD furnace, we can grow h-BN and graphene sequentially *in situ* in a high-quality synthesis that involves no transfer processes. Our experimental results show that Cu foil covered with an h-BN film of a limited thickness (the maximum value was about 4 nm in our experiments) can catalyze the decomposition of methane and the growth of graphene, in conflict with a general perception that only exposed Cu surfaces have catalytic properties with respect to graphene growth in low-pressure CVD systems. The catalytic effects of h-BN/Cu are much stronger than those of bulk h-BN and weaker than those of Cu and decrease with increasing thickness of the h-BN film. As reported in our previous paper,

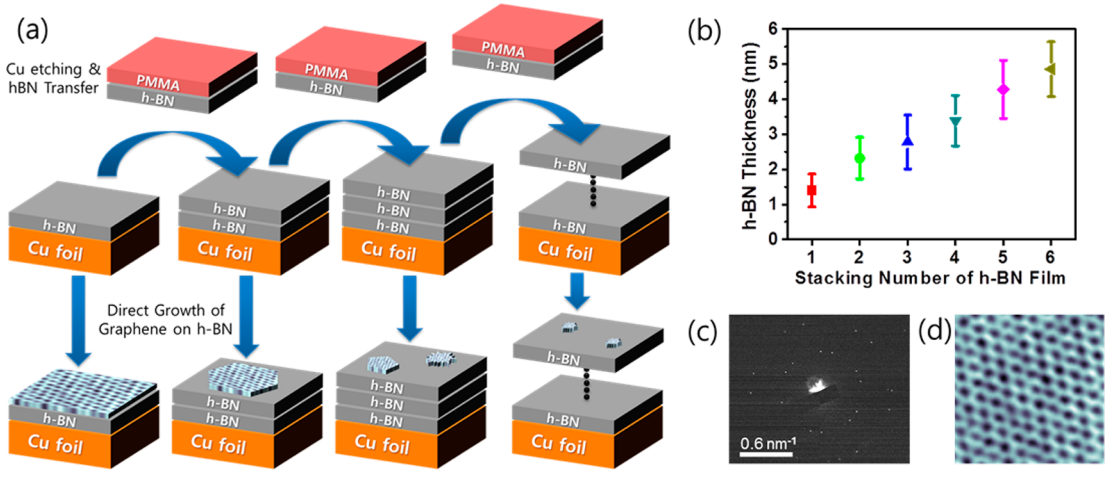

Figure 1. (a) Diagrams of the growth of CVD graphene on stacks of large-area CVD h-BN films with different thicknesses; (b) plot of the total thicknesses of h-BN *vs* the total number of h-BN films transferred with PMMA; (c) SAED diffraction pattern with peaks due to graphene and the h-BN film; (d) high-resolution scanning tunneling microscopy image of graphene on an h-BN film. Panels (c) and (d) were obtained for a sample consisting of graphene on one h-BN film without additional h-BN films.

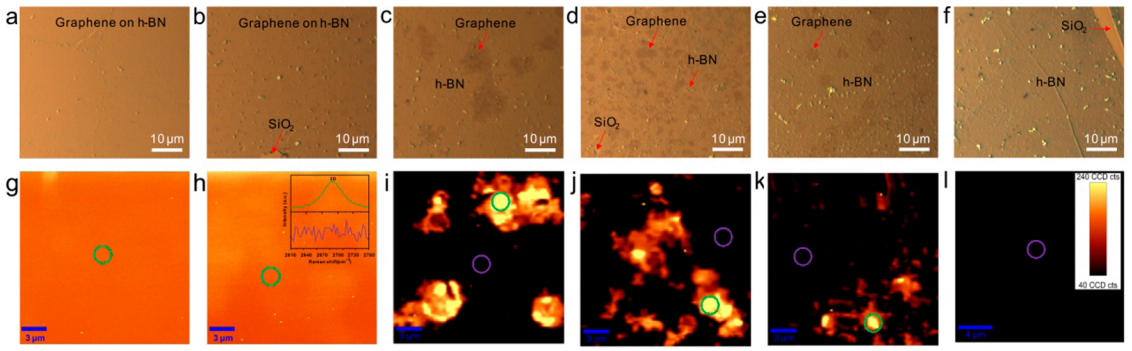

Figure 2. (a−f) Optical microscopy images of graphene/BN samples after transfer onto 90 nm SiO_2/Si substrates from a Cu foil with 1 to 6 h-BN films. Uniform and continuous graphene is present in (a) and (b), discontinuous graphene with a size of several micrometers is present in (c), (d), and (e), and no graphene is present in (f). (g−l) Corresponding Raman maps of the 2D (2660 to 2720 cm^{-1}) bands of the graphene/h-BN with corresponding number of h-BN films. (Inset) 2D peak from the marked spots with corresponding colored circles (green and purple) shows the existence of graphene.

when a thin h-BN film (thickness about 2 nm) is present on a Cu foil, the typical domain size of the graphene grown on the h-BN/Cu foil is up to 30 μm, which is comparable to that of graphene grown on Cu foil under the same conditions and 3 orders of magnitude larger than that of graphene grown on SiO_2, Si_3N_4, and h-BN.[13−17,22] Approximately 93% of the graphene film grown on h-BN/Cu foil exhibits a peak intensity ratio of $I_D/I_G < 0.2$,[12] which is much smaller than that for the few layers of graphene grown on h-BN powders and h-BN/Al_2O_3.[23,24] The SAED diffraction patterns and STM images (Figures 1c,d) show that the graphene grown on a single h-BN film has high crystallinity over a large area.

The main focus of this study was to determine the mechanism of the catalytic growth of graphene on h-BN/Cu by examining the dependence of the thickness of the h-BN film on the graphene growth. To change the thickness of the h-BN films, we grew h-BN films on a Cu foil and transferred these h-BN films onto other h-BN/Cu foils as required (Figure 1b).

With this method, we were able to obtain a uniform and continuous multilayer stack of large-area CVD-grown h-BN films with controlled thicknesses. The thickness of each h-BN film was measured with atomic force microscopy (AFM). As expected, the thickness of a multilayer stack of h-BN films increases linearly with the number of h-BN films in the stack, as shown in Figure 1b. These multilayer stacks of h-BN films with various thicknesses on a Cu foil were used as substrates for graphene growth. Figure 2a−f show optical microscopy (OM) images of the graphene samples grown on h-BN and transferred to SiO_2. Graphene growth was further confirmed through Raman mapping of the 2D (2660 to 2720 cm^{-1}) bands to identify the graphene and non-graphene areas on our samples, as shown in Figure 2g−l. In Figure 2g and h, a stack of 1 and 2 h-BN films is covered with continuous graphene. Figure 2i−k for a multilayer stack of 3, 4, and 5 h-BN films show partial growth of micrometer-sized graphene, but no graphene was detected on a stack of 6 h-BN films, as shown in Figure 2l. Although alignment or rotation between h-BN films in the stack was not controllable, no significant difference of graphene quality was observed on different h-BN regions of the same thickness in the same Cu foil sample.

From Figure 2 it can be seen that the catalytic properties of h-BN/Cu are strongly dependent on the h-BN thickness and are very different from those of the bulk h-BN. These catalytic properties were investigated further by measuring the surface potentials of films with Kelvin probe force microscopy. For this purpose, h-BN platelets with different thicknesses were produced by mechanically exfoliating h-BN flakes onto SiO_2. Figure 3a−c show AFM images of three different h-BN platelets with different thickness distributions. In these images, the dark regions are SiO_2 and thicker h-BN regions produce a brighter contrast. The corresponding Raman mappings of the h-BN peaks for those three locations were also carefully measured and are shown in Figure 3d−f. Although some clear contrast differences are evident, the vertical resolution (contrast resolution) of the different h-BN thicknesses is not sufficient to distinguish between different numbers of atomic layers of h-BN. Figure 3g−i show the corresponding KPFM images of all three locations. The bare SiO_2 surface produces the brightest contrast, and the thicker h-BN film looks darker, which indicates that the catalytic effects of the Cu foil become weaker for thicker dielectric layers. More analytical information is shown in Figure 3j, in which the surface potential differences with respect to the base SiO_2 surface are plotted for many different h-BN thicknesses from 0 to 15 nm. The curve fitted to these data (the red solid line) clearly shows the exponential dependence of the surface potential difference on h-BN thickness. This result implies that charge transfer through the h-BN film from the Cu foil is essential to the catalytic properties of the h-BN film surface, which are thus very different from those of bulk h-BN surfaces.

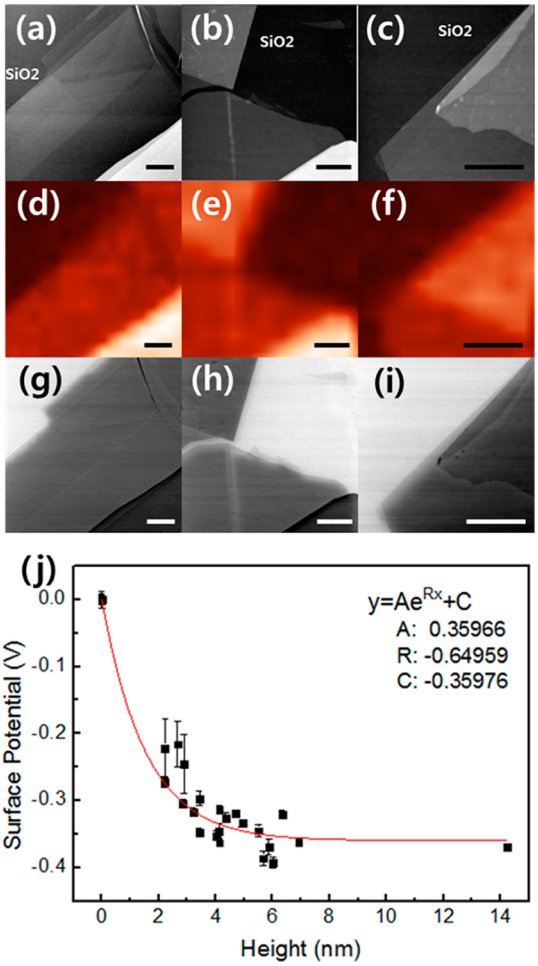

Figure 3. (a–c) AFM images of exfoliated h-BN platelets from different locations on the SiO_2 substrate, (d–f) Raman maps of the h-BN peaks (1327–1378 cm^{-1}, h-BN peak at 1352 cm^{-1}) of (a)–(c), and (g–i) the corresponding KPFM images. (j) Plot of the surface potential differences with respect to SiO_2, measured for (g)–(i). All the scale bars in (a)–(i) are 1 μm.

First-principles DFT calculations were conducted to clarify the role of the copper metal underlying the h-BN film and the film thickness of h-BN in the binding of carbon sources onto h-BN/Cu(111). First we first explored the binding strength of the CH_3 radical (formed after the desorption of H_2 from methane molecules, CH_4) on the bare (111) Cu surface and on free-standing h-BN. The optimized geometries are illustrated in Figure 4a and b, respectively; a single CH_3 adsorbate was modeled as a precursor for the exploration of binding affinity. Figure 4c–e show systems composed of one, two, and three atomic layers of h-BN on a Cu(111) surface. In Figure 4f–j, the potential energy curves with respect to the distance between CH_3 and the surface are shown in solid symbols. The Bader charge of the carbon atom in CH_3 is also shown by the open symbols. Figure 4h–j show the partial electron transfer from the underlying Cu to CH_3 when it approaches the h-BN surface. Such electron transfer is negligible when CH_3 is present on the bare Cu or on h-BN without Cu, as shown in Figure 4f and g, respectively. The binding energy at the equilibrium distance (1.98 Å) between CH_3 and the Cu surface was found to be approximately −2.2 eV (Figure 4f). The h-BN is a wide-band-gap insulator and is thus expected to be an inactive catalyst for adsorbates, as found in our computations for CH_3 on pristine h-BN, which are shown in Figure 4b and g. In contrast to pristine h-BN, the presence of Cu metal underneath leads to strong chemical bonding between CH_3 and h-BN with a binding energy of approximately −1.7 eV at an equilibrium separation of 1.65 Å (Figure 4h). This result clearly indicates that the presence of the metallic substrate greatly increases the catalytic activity and is thus believed to be the main origin of the easy growth of graphene on h-BN/Cu. Furthermore, our detailed analyses of the Bader charge reveal that the catalytic affinity of h-BN/Cu is due to charge transfer from the copper foil to carbon through the h-BN insulating layer (Figure 4h) and the induced polaronic distortions of the outer surface of the h-BN thin film (see Figure 4c).

The calculated binding energies for CH_3 on h-BN films consisting of two and three atomic layers on a Cu foil were found to be approximately −0.5 eV at 1.72 Å (Figure 4i) and −0.3 eV at 1.78 Å (Figure 4j), respectively. The charge accumulation at the carbon atom in CH_3 decreases as the h-BN film thickness increases, when the binding strength of CH_3 on h-BN/Cu is moderate. Figure 5 shows plots of the potential depth and the C atom Bader charge of CH_3 for h-BN films with different numbers of h-BN atomic layers on a Cu substrate. The potential depth decreases and saturates to zero, as the thickness of the h-BN film is increased to one, two, and three atomic layers. The potential depth of CH_3 on a bare Cu surface is not significantly different from that on one atomic layer of h-BN with underlying Cu. That such a thin h-BN film on Cu does not impede subsequent CVD growth of graphene means a new CVD template on which to directly grow large-area and high-quality graphene, thus having a particularly clean interface with the h-BN. Experiments showed that some patches of graphene can be grown even on h-BN films with thicknesses up to 4 nm, which is likely due to leakage of charge from the Cu substrate through the grain boundaries of the imperfect h-BN film. Thus, the mechanism of the catalytic growth of graphene on thin films of h-BN on a Cu substrate is completely different from the mechanism for (possible) growth on bulk-like h-BN.

CONCLUSION

Herein, our experimental and theoretical results show that the catalytic activation of h-BN by the underlying Cu plays a role in determining the nature of the bond between the carbon-containing precursor(s) and the h-BN that can yield surface-mediated growth of graphene. There is no need for a trade-off

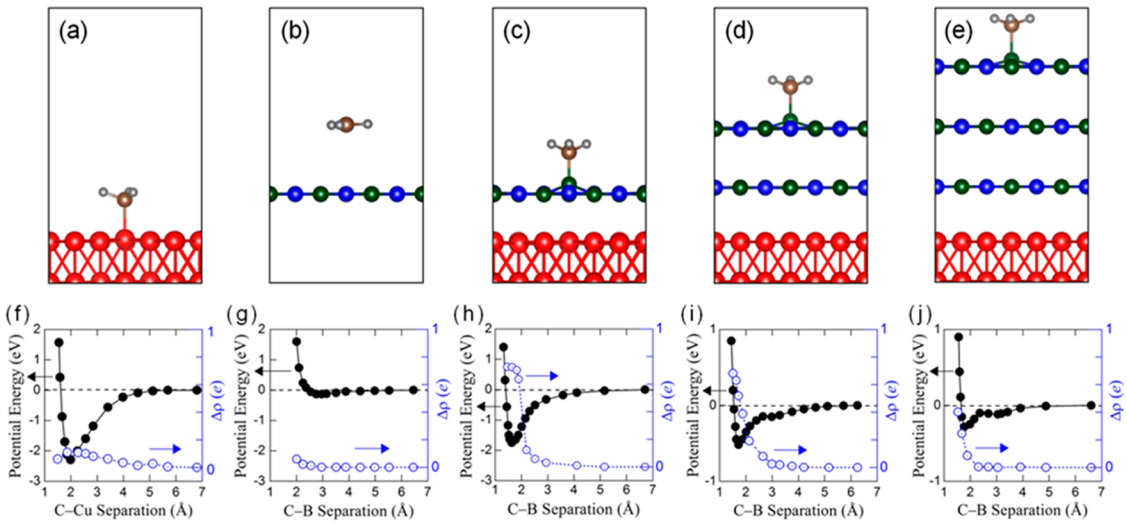

Figure 4. Optimized geometries, binding energy, and electron charge of the CH_3 radical on various adsorbents: (a and f) on the bare Cu(111) surface, (b and g) on free-standing h-BN, and (c–e, h, and i) on 1, 2, and 3 atomic layers of h-BN on Cu(111), respectively. The potential energy and charge profiles are given with respect to the distance between the C atom and an underlying atom of the substrate. CH_3 is adsorbed on top of a Cu atom in (a), whereas it sits on a B atom in (c), (d), and (e). The carbon and hydrogen atoms in CH_3 are depicted as big brown and small gray balls, respectively. The green and blue balls are the boron and nitrogen atoms of h-BN, and the red balls are copper atoms in the substrate. The electron charge of CH_3 was obtained through the Bader charge analysis of the C atom, and the presented data are defined as $\Delta\rho = \rho(CH_3/\text{adsorbent}) - \rho(\text{isolated } CH_3)$.

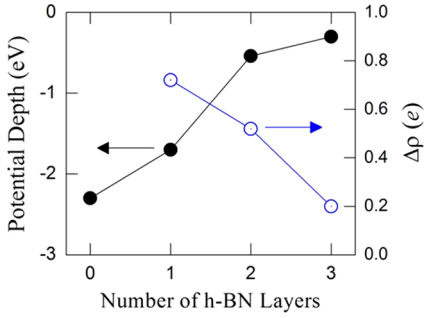

Figure 5. Potential depth (solid circles) and charge profile (open circles) of CH_3 on h-BN/Cu(111) *vs* the number of h-BN atomic layers. Zero h-BN layer is the bare Cu(111). The electron charge of CH_3 ($\Delta\rho$) is defined in the Figure 4 caption.

between the quality of either the graphene or the graphene/h-BN interface and the scalability, which we suggest may have a large impact on further studies of graphene on h-BN as well as the scaled production of the graphene-on-hBN material for a wide range of applications.

Perhaps of equal or greater importance is the realization that such ultrathin films on metal substrates can be essentially "transparent" in terms of the catalytic activity of the underlying metal but also protect the neat metal substrate and that growth of a wide variety of materials on top of them will be possible because of the influence of the underlying metal surface. For example, there is a need to grow the metal dichalcogenides of different types on h-BN for evaluation of new types of nanoelectronic devices. One can also imagine a wide range of fundamental studies involving patterning of the ultrathin film to, for example, different thicknesses and of the use of metal substrates having patterns of different and immiscible metals (at growth temperatures) that are protected by ultrathin layers deposited onto them.

METHODS

Synthesis. The synthesis of each h-BN film on Cu foil was carried out in a low-pressure CVD system. A 75 μm thick Cu foil placed in the CVD chamber was gradually heated to 1000 °C within 1 h in a gas mixture of 20 sccm Ar and 5 sccm H_2 and at a low pressure of 6 mTorr evacuated with a turbo pump and then annealed for 30 min under these conditions. h-BN growth was carried out for 10 min after introducing 1 sccm of borazine (kept in a water chiller at a temperature of −15 °C) carried in 2 sccm N_2.

Computation. We performed first-principles density-functional theory calculations by using the Vienna *ab initio* Simulation Package (VASP). The energy cutoff for the plane-wave basis was set at 400 eV, and the generalized gradient approximation formulated by Perdew, Burke, and Ernzerhof was used to describe the electron exchange correlation potential.[25,26] All DFT calculations in this work include the van der Waals energy by using the semiempirical form of DFT-D2, suggested by Grimme *et al.*[27] To simulate the BN-covered Cu surfaces, we set up a supercell that contains an h-BN film slab adsorbed on two layers of Cu, which was separated from its replica image by a large vacuum region of 15 Å. For the in-plane lattice, we used a (4×4) h-BN unit cell on the (4×4) Cu(111) supercell with periodic boundary conditions, and the atomic structures of h-BN on Cu were relaxed in the supercell. When the h-BN and Cu layers are relaxed independently, the lattice mismatch was found to be only 2%. We also investigated the electronic structure of the optimized h-BN and a Cu layer each and found that the effect of the 2% constraint on both lattices is negligible. A 3×3 *k*-point mesh from the Monkhorst–Pack scheme was sampled for integration over the two-dimensional

Brillouin zone. The experimental lattice constant (2.55 Å) of the (111) plane of Cu was used for the in-plane lattice in all the calculations. In the binding curve computations, only the hydrogen atoms of CH_3 and an underlying B atom on the substrate were allowed to relax for a given distance; other atoms were fixed at the optimized geometry corresponding to the most stable configuration of CH_3 on top of a B atom in h-BN/Cu.

Conflict of Interest: The authors declare no competing financial interest.

Acknowledgment. This research was supported by Basic Science Research Program through the National Research Foundation of Korea (NRF) funded by the Korean government (MSIP) (grant numbers: 2009-0083540, 2011-0030046, 2012R1A1A2020089, and 2012R1A1A1041416).

Supporting Information Available: The experimental methods to grow graphene directly on h-BN/Cu foil with different h-BN thicknesses are discussed in detail. This material is available free of charge *via* the Internet at http://pubs.acs.org.

REFERENCES AND NOTES

1. Li, X.; Cai, W.; An, J.; Kim, S.; Nah, J.; Yang, D.; Piner, R.; Velamakanni, A.; Jung, I.; Tutuc, E.; *et al*. Large-Area Synthesis of High-Quality and Uniform Graphene Films on Copper Foils. *Science* **2009**, *324*, 1312–1314.
2. Kim, K. S.; Zhao, Y.; Jang, H.; Lee, S. Y.; Kim, J. M.; Kim, K. S.; Ahn, J.-H.; Kim, P.; Choi, J.-Y.; Hong, B. H. Large-Scale Pattern Growth of Graphene Films for Stretchable Transparent Electrodes. *Nature* **2009**, *457*, 706–710.
3. Reina, A.; Jia, X.; Ho, J.; Nezich, D.; Son, H.; Bulovic, V.; Dresselhaus, M. S.; Kong, J. Large Area, Few-Layer Graphene Films on Arbitrary Substrates by Chemical Vapor Deposition. *Nano Lett.* **2009**, *9*, 30–35.
4. Song, L.; Ci, L.; Lu, H.; Sorokin, P. B.; Jin, C.; Ni, J.; Kvashnin, A. G.; Kvashnin, D. G.; Lou, J.; Yakobson, B. I.; *et al*. Large Scale Growth and Characterization of Atomic Hexagonal Boron Nitride Layers. *Nano Lett.* **2010**, *10*, 3209–3215.
5. Lee, K. H.; Shin, H.-J.; Lee, J.; Lee, I.; Kim, G.-H.; Choi, J.-Y.; Kim, S.-W. Large-Scale Synthesis of High-Quality Hexagonal Boron Nitride Nanosheets for Large-Area Graphene Electronics. *Nano Lett.* **2012**, *12*, 714–718.
6. Shi, Y.; Hamsen, C.; Jia, X.; Kim, K. K.; Reina, A.; Hofmann, M.; Hsu, A. L.; Zhang, K.; Li, H.; Juang, Z.-Y.; *et al*. Synthesis of Few-Layer Hexagonal Boron Nitride Thin Film by Chemical Vapor Deposition. *Nano Lett.* **2010**, *10*, 4134–4139.
7. Kim, K. K.; Hsu, A.; Jia, X.; Kim, S. M.; Shi, Y.; Hofmann, M.; Nezich, D.; Rodriguez-Nieva, J. F.; Dresselhaus, M.; Palacios, T.; *et al*. Synthesis of Monolayer Hexagonal Boron Nitride on Cu Foil Using Chemical Vapor Deposition. *Nano Lett.* **2012**, *12*, 161–166.
8. Joshi, S.; Ecija, D.; Koitz, R.; Iannuzzi, M.; Seitsonen, A. P.; Hutter, J.; Sachdev, H.; Vijayaraghavan, S.; Bischoff, F.; Seufert, K.; *et al*. Boron Nitride on Cu(111): An Electronically Corrugated Monolayer. *Nano Lett.* **2012**, *12*, 5821–5828.
9. Gao, Y.; Ren, W.; Ma, T.; Liu, Z.; Zhang, Y.; Liu, W.-B.; Ma, L.-P.; Ma, X.; Cheng, H.-M. Repeated and Controlled Growth of Monolayer, Bilayer and Few-Layer Hexagonal Boron Nitride on Pt Foils. *ACS Nano* **2013**, *7*, 5199–5206.
10. Dean, C. R.; Young, A. F.; Meric, I.; Lee, C.; Wang, L.; Sorgenfrei, S.; Watanabe, K.; Taniguchi, T.; Kim, P.; Shepard, K. L.; *et al*. Boron Nitride Substrates for High-Quality Graphene Electronics. *Nat. Nanotechnol.* **2010**, *5*, 722–726.
11. Xue, J.; Sanchez-Yamagishi, J.; Bulmash, D.; Jacquod, P.; Deshpande, A.; Watanabe, K.; Taniguchi, T.; Jarillo-Herrero, P.; LeRoy, B. J. Scanning Tunnelling Microscopy and Spectroscopy of Ultra-Flat Graphene on Hexagonal Boron Nitride. *Nat. Mater.* **2011**, *10*, 282–285.
12. Wang, M.; Jang, S. K.; Jang, W.-J.; Kim, M.; Park, S.-Y.; Kim, S.-W.; Kahng, S.-J.; Choi, J.-Y.; Ruoff, R. S.; Song, Y. J.; *et al*. A Platform for Large-Scale Graphene Electronics – CVD Growth of Single-Layer Graphene on CVD-Grown Hexagonal Boron Nitride. *Adv. Mater.* **2013**, *25*, 2746–2752.
13. Zhang, L.; Shi, Z.; Wang, Y.; Yang, R.; Shi, D.; Zhang, G. Catalyst-Free Growth of Nanographene Films on Various Substrates. *Nano Res.* **2011**, *4*, 315–321.
14. Rümmeli, M. H.; Bachmatiuk, A.; Scott, A.; Börrnert, F.; Warner, J. H.; Hoffman, V.; Lin, J.-H.; Cuniberti, G.; Büchner, B. Direct Low-Temperature Nanographene CVD Synthesis over a Dielectric Insulator. *ACS Nano* **2010**, *4*, 4206–4210.
15. Medina, H.; Lin, Y.-C.; Jin, C.; Lu, C.-C.; Yeh, C.-H.; Huang, K.-P.; Suenaga, K.; Robertson, J.; Chiu, P.-W. Metal-Free Growth of Nanographene on Silicon Oxides for Transparent Conducting Applications. *Adv. Funct. Mater.* **2012**, *22*, 2123–2128.
16. Chen, J.; Wen, Y.; Guo, Y.; Wu, B.; Huang, L.; Xue, Y.; Geng, D.; Wang, D.; Yu, G.; Liu, Y. Oxygen-Aided Synthesis of Polycrystalline Graphene on Silicon Dioxide Substrates. *J. Am. Chem. Soc.* **2011**, *133*, 17548–17551.
17. Chen, J.; Guo, Y.; Wen, Y.; Huang, L.; Xue, Y.; Geng, D.; Wu, B.; Luo, B.; Yu, G.; Liu, Y. Two-Stage Metal-Catalyst-Free Growth of High-Quality Polycrystalline Graphene Films on Silicon Nitride Substrates. *Adv. Mater.* **2013**, *25*, 992–997.
18. Yang, W.; Chen, G.; Shi, Z.; Liu, C.-C.; Zhang, L.; Xie, G.; Cheng, M.; Wang, D.; Yang, R.; Shi, D.; *et al*. Epitaxial Growth of Single-Domain Graphene on Hexagonal Boron Nitride. *Nat. Mater.* **2013**, *12*, 792–797.
19. Liu, Z.; Song, L.; Zhao, S.; Huang, J.; Ma, L.; Zhang, J.; Lou, J.; Ajayan, P. M. Direct Growth of Graphene/Hexagonal Boron Nitride Stacked Layers. *Nano Lett.* **2011**, *11*, 2032–2037.
20. Levendorf, M. P.; Kim, C.-J.; Brown, L.; Huang, P. Y.; Havener, R. W.; Muller, D. A.; Park, J. Graphene and Boron Nitride Lateral Heterostructures for Atomically Thin Circuitry. *Nature* **2012**, *488*, 627–632.
21. Liu, Z.; Ma, L.; Shi, G.; Zhou, W.; Gong, Y.; Lei, S.; Yang, X.; Zhang, J.; Yu, J.; Hackenberg, K. P.; *et al*. In-Plane Heterostructures of Graphene and Hexagonal Boron Nitride with Controlled Domain Sizes. *Nat. Nanotechnol.* **2013**, *8*, 119–124.
22. Tang, S.; Ding, G.; Xie, X.; Chen, J.; Wang, C.; Ding, X.; Huang, F.; Lu, W.; Jiang, M. Nucleation and Growth of Single Crystal Graphene on Hexagonal Boron Nitride. *Carbon* **2012**, *50*, 329–331.
23. Lin, T.; Wang, Y.; Bi, H.; Wan, D.; Huang, F.; Xie, X.; Jiang, M. Hydrogen Flame Synthesis of Few-Layer Graphene from a Solid Carbon Source on Hexagonal Boron Nitride. *J. Mater. Chem.* **2012**, *22*, 2859–2862.
24. Kim, K.; Choi, J.-Y.; Kim, T.; Cho, S.-H.; Chung, H.-J. A Role for Graphene in Silicon-Based Semiconductor Devices. *Nature* **2011**, *479*, 338–344.
25. Kresse, G.; Furthmüller, J. Efficient Iterative Schemes for ab Initio Total-Energy Calculations Using a Plane-Wave Basis Set. *Phys. Rev. B* **1996**, *54*, 11169–11186.
26. Perdew, J. P.; Burke, K.; Ernzerhof, M. Generalized Gradient Approximation Made Simple. *Phys. Rev. Lett.* **1996**, *77*, 3865–3868.
27. Grimme, S. Semiempirical GGA-Type Density Functional Constructed with a Long-Range Dispersion Correction. *J. Comput. Chem.* **2006**, *27*, 1787–1799.